JACS
JOURNAL OF THE AMERICAN CHEMICAL SOCIETY
Communication
pubs.acs.org/JACS

Highly Efficient Dual-Color Electrochemiluminescence from BODIPY-Capped PbS Nanocrystals

Mahdi Hesari,[†,∥] Kalen N. Swanick,[†,∥] Jia-Sheng Lu,[‡] Ryan Whyte,[†] Suning Wang,[*,‡,§] and Zhifeng Ding[*,†]

[†]Department of Chemistry, The University of Western Ontario, London, ON N6A 5B7, Canada
[‡]Department of Chemistry, Queen's University, Kingston, ON K7L 3N6, Canada
[§]Beijing Key Laboratory of Photoelectronic/Electrophotonic Conversion Materials, School of Chemistry, Beijing Institute of Technology, Beijing 100081, P. R. China

Supporting Information

ABSTRACT: Electrochemiluminescence (ECL) of a hybrid system consisting of PbS nanocrystals (NCs) and a BODIPY dye (BDY) capping ligand was discovered to produce highly efficient dual emissions with tri-*n*-propylamine as a coreactant. By means of spooling ECL spectroscopy, the strong dual ECL emission peaks of 984 and 680 nm were attributed to the PbS and BDY moieties, respectively, and found to be simultaneous during the light evolution and devolution. The ECL of the PbS was enhanced via NC collisions with the electrode and reached an efficiency of 96% relative to that of $Ru(bpy)_3^{2+}$, which is the highest among the semiconductor NCs.

Ding et al. demonstrated electrochemiluminescence or electrogenerated chemiluminescence (ECL)[1] of silicon nanocrystals[2] (NCs) a decade ago. Since then, a wide range of semiconductor NCs[3] such as Ge,[4] CdTe,[5] CdSe,[6] CdSe/ZnSe,[7] and PbS,[8] as well as carbon NCs[9] have been investigated for the ECL in visible or near-infrared (NIR) region.[8,10] In most cases, the inherent optical and electrochemical properties do not translate into efficient ECL, due to the surface state induction effect.[3,11] For example, it has been shown that replacing oleic acid (OA) with octadecylamine can change the ECL of PbS QDs, although it is still weak emission.[12]

Bard, Rosenthal, and co-workers pioneered the electrochemistry and ECL research of several BODIPY dyes in aqueous,[13] organic,[14] and emulsion[15] media. In all cases, the electrochemical features showed a direct correlation to the BODIPY structures,[16] while their ECL efficiency was not as high as expected. Our designed BODIPY dye (BDY, Scheme 1) that has a giant molecular structure is chemically and electrochemically stable, with a photoluminescence (PL) quantum yield of 0.24 vs. rhodamine B,[17] and an efficient ECL efficiency of >80% relative to that of $Ru(bpy)_3^{2+}$/TPrA coreactant system.[18] PbS NCs emit in NIR region, which is suitable for *in vivo*[19] or *in vitro* bioimaging[20] and applications in medical sciences.[21] The visible light emission of the BDY moiety is readily visualized by the naked eyes. The combination of both the PbS and BDY in the same system could enable dual emissive ECL systems, which have not been demonstrated before.

Herein, for the first time we report highly efficient dual-color ECL based on a PbS and BDY hybrid system (PbS-BDY, Schemes 1 and S1 in Supporting Information) in the presence of tri-*n*-propylamine (TPrA) as a reductive coreactant. Spooling ECL spectroscopy[18,22] of PbS-BDY and PbS-OA along with the ECL−voltage curve was used in elucidating the ECL mechanisms.

PbS-BDY and PbS-OA NCs were synthesized according to procedures reported by us elsewhere.[17] Figure 1a shows the spooling ECL spectra of 0.3 mg/mL PbS-BDY NCs with 20 mM TPrA in CH_2Cl_2 during a potential scan cycle between −0.4 and 1.4 V vs. SCE at 20 mV s^{-1}. The ECL spectrum of PbS-BDY shows two nominal peaks at 680 and 984 nm at an onset potential of 0.540 V (Figure S1a in Supporting Information). In contrast, the onset ECL spectrum of PbS-OA NCs under the same conditions displays only one emission peak at 975 nm at approximately the same potential (0.560 V, Figures 1b and S1b). The differential pulse voltammogram (DPV) of the PbS-BDY (Figure 2a) shows a nominal peak at 0.744 V vs. SCE, corresponding to the generation of $PbS^{\bullet+}$-$BDY^{\bullet+}$ (BDY is oxidized at 0.603 V[18]), while that of PbS-OA displays an oxidation reaction to $PbS\text{-}OA^{\bullet+}$ with a peak potential (E_p) of 0.685 V (Figure 2b). Relevant cyclic voltammograms are also provided in Figures S2 and S3. At the ECL onset potential, both the oxidized PbS and BDY moieties reacted with the electrogenerated ($E_p \approx 0.81$ V vs. SCE) $TPrA^{\bullet}$[23] that has a reduction power of −1.7 eV, injecting an electron to their LUMOs, as illustrated in Scheme 1.

These electron transfer reactions led to the formation of excited PbS (PbS*) (Scheme 1a) and BDY (BDY*) species (Scheme 1b) that relaxed to the ground state and emitted light simultaneously. It is also very possible that the two excited states are generated on the same nanocrystal because of the close oxidation potentials of the BDY and PbS. The evolution and devolution of the two ECL emissions during the potential scan cycle followed the reaction kinetics of the system (Figure 1a) and did not change the peak wavelengths, which are parallel to those of PbS-OA (Figure 1b) and BDY[18] luminophores and

Received: July 22, 2015
Published: August 26, 2015

DOI: 10.1021/jacs.5b07633
J. Am. Chem. Soc. 2015, 137, 11266−11269

Scheme 1. ECL Mechanisms of PbS-BDY Nanocrystals in the Presence of TPrA

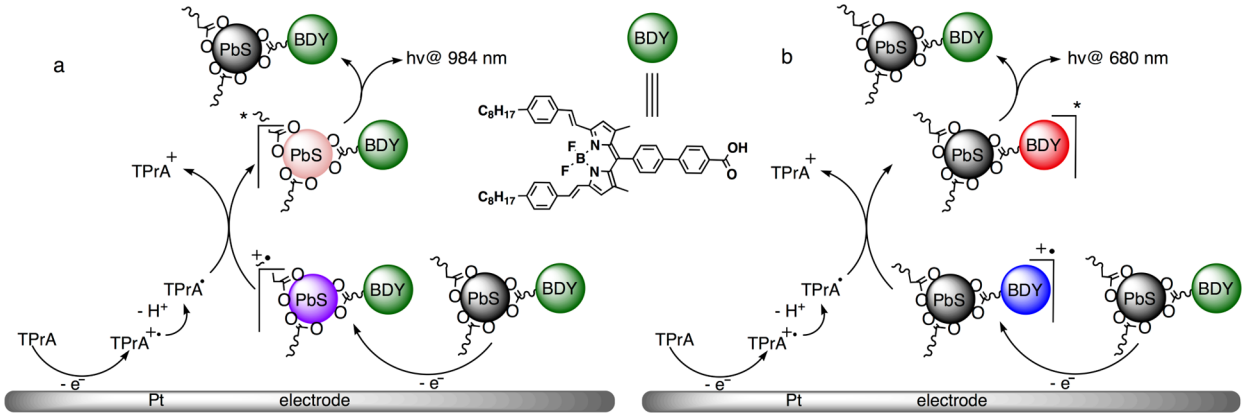

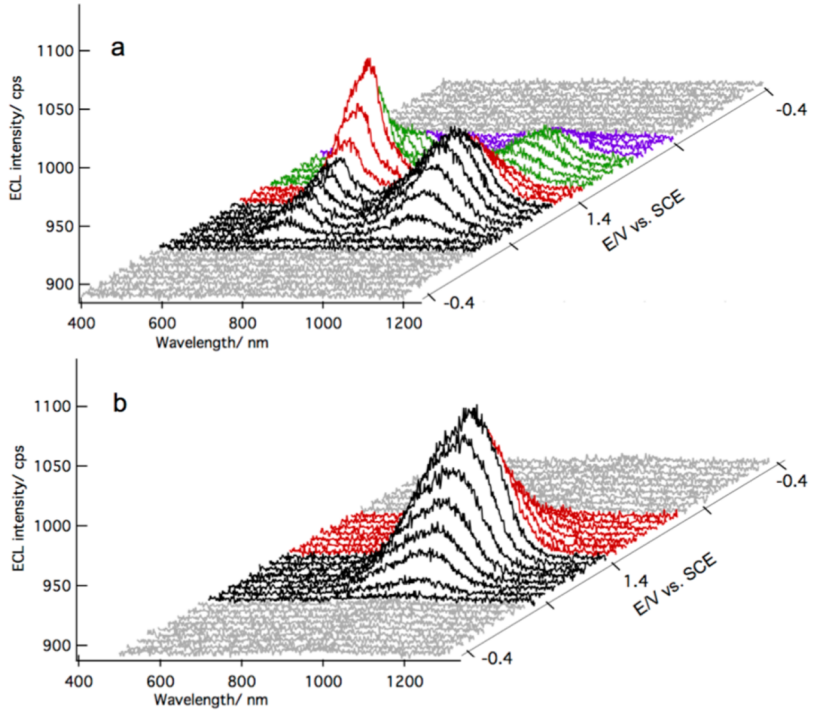

Figure 1. Spooling ECL spectra of (a) 0.3 mg/mL PbS-BDY and (b) 0.3 mg/mL PbS-OA NCs in CH_2Cl_2 containing 0.1 M $TBAPF_6$ during a potential scan cycle between −0.4 and 1.4 V vs SCE at a scan rate of 20 mV s^{-1}. Each spectrum was acquired for 1 s, with a time interval of 5 s.

agree very well with those determined from ECL−voltage curves (Supporting Information).

The ECL peak at 984 nm was assigned to the PbS moiety, while that at 679 nm to the BDY site by comparing the ECL spectra of the PbS-BDY, PbS-OA (Figure S1), and BDY.[18] These assignments were further corroborated by analyzing the photophysical properties of BDY,[18] PbS-OA, and PbS-BDY NCs along with the accumulated ECL spectra of the three systems (Figure 3). Under the irradiation of a 532 nm laser and with the same spectrograph and CCD camera apparatus as depicted elsewhere for Au nanoclusters,[22d] the PbS-BDY NCs showed a dual-color photoluminescence (PL) spectrum in both visible and NIR regions, dashed curve in Figure 3a. The weak PL peak at 955 nm in the NIR region correlates well with that of PbS-OA, shown in Figure 3b. In the visible region, the PbS-BDY NCs in CH_2Cl_2 display similar dual PL peaks as in toluene:[17] one from the relaxed excited state across the HOMO−LUMO gap (530 nm) and the other from interligand interactions (655 nm) similar to those (603 and 695 nm) of BDY.[18] The lower ECL intensity at 984 nm from the PbS-BDY (Figure 1a) than that of the PbS-OA (Figure 1b) was due to the lower nominal PbS concentration in the PbS-BDY than that in the PbS-OA, when the same mass concentration of 0.33 mg/mL was used, assuming PbS NC size unchanged during the PbS-BDY preparation via ligand exchange from OA to BDY.[17] The small red shift of the ECL peak relative to the PL one is attributed to the inner-filter effect.[16b] Interestingly, the BDY ECL peak of the PbS-BDY (red in Figure 3a) shows a shoulder peak at ∼615 nm, which was not observed in the ECL of the BDY electrolyte solution.[18] Deconvolution of the spooling spectra at 1.1 and 1.4 V vs. SCE is shown in Figure S4 with three fitted peaks at 615, 687, and 984 nm. The dominance of the 687 nm emission peak of PbS-BDY in the ECL spectrum indicated that the intermolecular interactions between the BDY ligands in PbS-BDY are very strong, similar to those of high concentration solutions of BDY.[18] This is understandable since

DOI: 10.1021/jacs.5b07633
J. Am. Chem. Soc. 2015, 137, 11266−11269

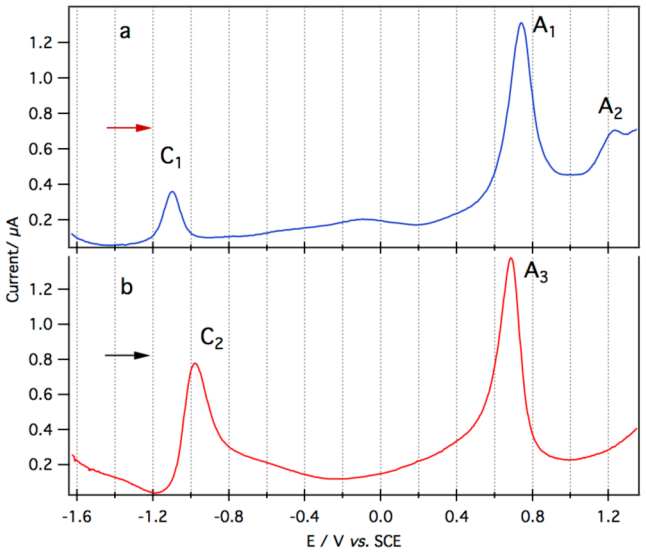

Figure 2. Differential pulse voltammograms (DPVs) of (a) PbS-BDY NCs (0.33 mg/mL) and (b) PbS-OA NCs (0.33 mg/mL) obtained in CH_2Cl_2 containing 0.1 M $TBAPF_6$.

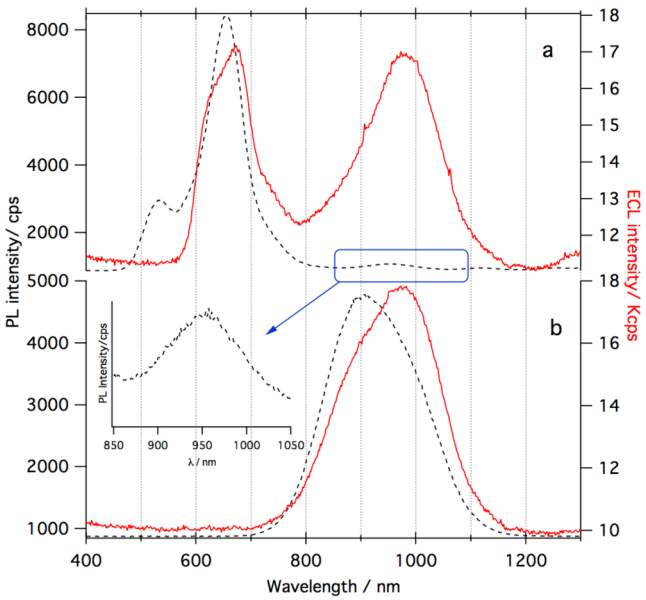

Figure 3. PL (dashed lines, excited at 532 nm) of PbS-BDY (a) and PbS-OA (b). The solid lines show accumulated ECL spectra of PbS-BDY/TPrA (a) and PbS-OA/TPrA (b). The ECL spectra were obtained during two consecutive potential scan cycles at 20 mV s^{-1} in the potential range of −0.4 to 1.4 V for both PbS-DBY/TPrA and PbS-OA/TPrA systems. The inset shows the zoomed-in part of the PL spectrum.

the PbS NCs act as an anchor to concentrated BDY ligands around the core, resulting in strong interligand $\pi-\pi$ interactions.

The dual ECL emissions of the PbS NC and BDY ligand were present throughout the entire ECL spooling experiment (Figures 1a and S5), while the peak intensities varied with the potential change. After the onset ECL spectrum (Figure S1a), the ECL emissions at 984 and 680 nm augment simultaneously (Figure S5a) with the potential moving to 1.1 V. This could be due to the close oxidation potentials for both PbS and BDY in the assembled hybrid system and the increase of the TPrA radial concentration. With the applied potential moving further positive (1.2 to 1.4 V, Figure S5b), the emissions from the two moieties increased while ECL intensity of BDY evolved more strongly than that of PbS. In the reverse scan from 1.3 to 0.9 V the PbS emission intensity remained constant; however, the BDY emission dropped gradually (Figure S5c). Finally, both ECL peak intensities decreased in the backward scan from 0.8 to 0.4 V, whereas BDY peak disappeared faster (dark-red and dark-orange curves in Figure S5d).

The ECL spectra of both the PbS-OA and PbS-BDY systems display a much stronger emission at 984 nm than their PL emission. These observations may be explained by collisional interactions of these NCs with the electrode surface that enhanced the electron transfer and the generation of the PbS radical cations because of the low band gap nature of the PbS core, which ultimately led to the ECL enhancement via the subsequent reaction of the PbS radical cations with TPrA radicals through the catalytic mechanisms established for the Pt NCs/$Ru(bpy)_3^{2+}$/TPrA system.[24] This might also be applicable to the ECL of ligand capped PbS QDs.[8]

The ECL from both the PbS-OA/TPrA and PbS-BDY/TPrA systems was investigated at other potential scan rates: 50, 100, and 200 mV s^{-1} (Figures S6–S11). The spooling ECL spectra in two consecutive cycles displayed a consistent pattern as described above. However, as the scan rate increased and the charge injection decreased, the peak heights decreased for both PbS and BDY emissions.

In the annihilation path, the PbS-BDY NCs did not show appreciable ECL during potential scanning in the range of 0.8 and −1.5 V (Figure 2) in which the radical cations and anions were believed to have been generated, while weak ECL emissions with the two peaks at 984 and 680 nm were recorded in the course of potential pulsing in the same range. ECL was observed mostly at the negative pulse limit (Figure S12a), revealing the higher cation stability compared to that of the anion one. Interestingly, the peak height at 984 nm in the accumulated ECL spectrum acquired during the potential pulsing in Figure S12b is weaker than the one at 680 nm. The above observation is in contrast to that in the coreactant route. This is probably due to the fast polarity change and short charge injection time during the pulsing and thus less ECL amplification of the PbS moiety in the collision events described above.

ECL efficiencies relative to $Ru(bpy)_3^{2+}$/TPrA[22a,b] for both PbS-OA and PbS-BDY NCs in the presence of TPrA at a potential scan rate of 20 mV s^{-1} were found to be almost as strong as the reference (Table S1) despite the overestimated consumed charge. The outstanding relative ECL efficiencies of the PbS in both PbS-BDY and PbS-OA systems up to 96% are the highest observed from the semiconductor NCs. The ECL efficiency of the PbS NCs decreased with an increase in scan rate, which is consistent with the ECL amplification via collisions with the electrode: the longer the charge injection time, the stronger the enhancement.

In conclusion, the PbS-BDY hybrid system is a strong dual-color ECL emitter in which the PbS moiety possesses the most efficient ECL among semiconductor NCs. NC collisional interactions with the electrode has been found to greatly enhance the ECL of the PbS moiety. The PbS-BDY system is anticipated to be excellent in biological imaging.[19b,20]

DOI: 10.1021/jacs.5b07633
J. Am. Chem. Soc. 2015, 137, 11266–11269

■ ASSOCIATED CONTENT

Supporting Information

The Supporting Information is available free of charge on the ACS Publications website at DOI: 10.1021/jacs.5b07633.

Additional ECL−voltage curves, spooling ECL spectra, and ECL efficiency calculations (PDF)

■ AUTHOR INFORMATION

Corresponding Authors

*zfding@uwo.ca

*wangs@chem.queensu.ca

Author Contributions

‖These authors contributed equally to this work.

Notes

The authors declare no competing financial interest.

■ ACKNOWLEDGMENTS

Authors acknowledge the financial support from NSERC, CFI, PREA, and Western and Queen's University. The quality service from our electronic shop and ChemBio Store at Western is well appreciated. We thank Ye Tao and his team at the National Research Council for providing the PbS-OA NCs.

■ REFERENCES

(1) (a) Bard, A. J. *Electrogenerated Chemiluminescence*; Marcel Dekker: New York, 2004. (b) Miao, W. *Chem. Rev.* **2008**, *108*, 2506−2553. (c) Richter, M. M. *Chem. Rev.* **2004**, *104*, 3003−3036.

(2) Ding, Z.; Quinn, B. M.; Haram, S. K.; Pell, L. E.; Korgel, B. A.; Bard, A. J. *Science* **2002**, *296*, 1293−1297.

(3) Bard, A.; Ding, Z.; Myung, N. *Struct. Bonding (Berlin)* **2005**, *118*, 1−57.

(4) Myung, N.; Lu, X.; Johnston, K. P.; Bard, A. J. *Nano Lett.* **2004**, *4*, 183−185.

(5) Bae, Y.; Myung, N.; Bard, A. J. *Nano Lett.* **2004**, *4*, 1153−1161.

(6) (a) Myung, N.; Ding, Z.; Bard, A. J. *Nano Lett.* **2002**, *2*, 1315−1319. (b) Zhou, J.; Zhu, J.; Brzezinski, J.; Ding, Z. *Can. J. Chem.* **2009**, *87*, 386−391.

(7) Myung, N.; Bae, Y.; Bard, A. J. *Nano Lett.* **2003**, *3*, 1053−1055.

(8) Sun, L.; Bao, L.; Hyun, B.-R.; Bartnik, A. C.; Zhong, Y.-W.; Reed, J. C.; Pang, D.-W.; Abruña, H. D.; Malliaras, G. G.; Wise, F. W. *Nano Lett.* **2009**, *9*, 789−793.

(9) (a) Zhou, J.; Booker, C.; Li, R.; Sun, X.; Sham, T.-K.; Ding, Z. *Chem. Phys. Lett.* **2010**, *493*, 296−298. (b) Zheng, L.; Chi, Y.; Dong, Y.; Lin, J.; Wang, B. *J. Am. Chem. Soc.* **2009**, *131*, 4564−4565.

(10) Wang, J.; Han, H. *Rev. Anal. Chem.* **2013**, *32*, 91−101.

(11) (a) Hines, D. A.; Kamat, P. V. *ACS Appl. Mater. Interfaces* **2014**, *6*, 3041−3057. (b) Patra, S.; Samanta, A. *J. Phys. Chem. C* **2014**, *118*, 18187−18196. (c) Kamat, P. V.; Christians, J. A.; Radich, J. G. *Langmuir* **2014**, *30*, 5716−5725.

(12) Bakueva, L.; Musikhin, S.; Hines, M. A.; Chang, T.-W. F.; Tzolov, M.; Scholes, G. D.; Sargent, E. H. *Appl. Phys. Lett.* **2003**, *82*, 2895−2897.

(13) Nepomnyashchii, A. B.; Pistner, A. J.; Bard, A. J.; Rosenthal, J. *J. Phys. Chem. C* **2013**, *117*, 5599−5609.

(14) (a) Nepomnyashchii, A. B.; Bröring, M.; Ahrens, J.; Bard, A. J. *J. Am. Chem. Soc.* **2011**, *133*, 8633−8645. (b) Qi, H.; Teesdale, J. J.; Pupillo, R. C.; Rosenthal, J.; Bard, A. J. *J. Am. Chem. Soc.* **2013**, *135*, 13558−13566.

(15) Dick, J. E.; Renault, C.; Kim, B.-K.; Bard, A. J. *J. Am. Chem. Soc.* **2014**, *136*, 13546−13549.

(16) (a) Nepomnyashchii, A. B.; Bard, A. J. *Acc. Chem. Res.* **2012**, *45*, 1844−1853. (b) Nepomnyashchii, A. B.; Cho, S.; Rossky, P. J.; Bard, A. J. *J. Am. Chem. Soc.* **2010**, *132*, 17550−17559.

(17) Lu, J.-S.; Fu, H.; Zhang, Y.; Jakubek, Z. J.; Tao, Y.; Wang, S. *Angew. Chem., Int. Ed.* **2011**, *50*, 11658−11662.

(18) Hesari, M.; Lu, J.-S.; Wang, S.; Ding, Z. *Chem. Commun.* **2015**, *51*, 1081−1084.

(19) (a) Corricelli, M.; Depalo, N.; Di Carlo, E.; Fanizza, E.; Laquintana, V.; Denora, N.; Agostiano, A.; Striccoli, M.; Curri, M. L. *Nanoscale* **2014**, *6*, 7924−7933. (b) Wang, D.; Qian, J.; Cai, F.; He, S.; Han, S.; Mu, Y. *Nanotechnology* **2012**, *23*, 245701.

(20) Oscar, B. G.; Liu, W.; Zhao, Y.; Tang, L.; Wang, Y.; Campbell, R. E.; Fang, C. *Proc. Natl. Acad. Sci. U. S. A.* **2014**, *111*, 10191−10196.

(21) Geszke-Moritz, M.; Moritz, M. *Mater. Sci. Eng., C* **2013**, *33*, 1008−1021.

(22) (a) Hesari, M.; Workentin, M. S.; Ding, Z. *Chem. Sci.* **2014**, *5*, 3814−3822. (b) Hesari, M.; Workentin, M. S.; Ding, Z. *ACS Nano* **2014**, *8*, 8543−8553. (c) Swanick, K. N.; Hesari, M.; Workentin, M. S.; Ding, Z. *J. Am. Chem. Soc.* **2012**, *134*, 15205−15208. (d) Hesari, M.; Workentin, M. S.; Ding, Z. *Chem. - Eur. J.* **2014**, *20*, 15116−15121. (e) Swanick, K. N.; Ladouceur, S.; Zysman-Colman, E.; Ding, Z. *Angew. Chem., Int. Ed.* **2012**, *51*, 11079−11082. (f) Swanick, K. N.; Sandroni, M.; Ding, Z.; Zysman-Colman, E. *Chem. - Eur. J.* **2015**, *21*, 7435−7440.

(23) (a) Lai, R. Y.; Bard, A. J. *J. Phys. Chem. A* **2003**, *107*, 3335−3340. (b) Miao, W.; Choi, J.-P.; Bard, A. J. *J. Am. Chem. Soc.* **2002**, *124*, 14478−14485. (c) Benoist, D. M.; Pan, S. J. *J. Phys. Chem. C* **2010**, *114*, 1815−1821.

(24) Fan, F.-R. F.; Bard, A. J. *Nano Lett.* **2008**, *8*, 1746−1749.

DOI: 10.1021/jacs.5b07633
J. Am. Chem. Soc. 2015, 137, 11266−11269